Synthesis and Characterization of Regiorandom and Regioregular Poly(3-octylfuran)

Jeffrey K. Politis, Joel C. Nemes, and M. David Curtis*

Contribution from the Willard H. Dow Laboratory, Department of Chemistry, and the Macromolecular Science and Engineering Program, The University of Michigan, Ann Arbor, Michigan 48109-1055

Received October 4, 2000

Abstract: Poly(3-octylfuran) has been synthesized with three regioregularities: **P3OF-95**, **P3OF-75**, and **P3OF-50**, where the number signifies the percentage HT content. The 95% HT material is highly crystalline with a structure similar to that of HT-poly(3-octylthiophene), **P3OT**. The lamellar spacing is 22.1 Å and the π-stacking distance is 3.81 Å. UV−vis spectroscopy reveals that **P3OF-95** is aggregated in $CHCl_3$ solution, and solid films of **P3OF-95**, but not **P3OF-75** or **-50**, show Davydov and exciton band splitting due to the interactions of the π-systems in the stacked morphology. An estimate of the Davydov splitting is 0.15 eV (1200 cm^{-1}). **P3OF** is reversibly oxidized at 0.32 V vs ferrocene/ferrocenium, but increasing the potential to 1.15 V leads to irreversible oxidation. Films of **P3OF** may be p-doped with iodine vapor. Doped **P3OF-95** and **-75** films have electrical conductivities of 10^{-2} and 10^{-7} S/cm, respectively. The UV−vis−NIR spectra of the iodine-doped films are interpreted in terms of molecular-like transitions involving the LUMO, HOMO, HOMO-1, and transitions across a Peierls distortion-induced gap in the intermolecular conduction band that is formed by the overlap of the π-systems of the stacked partially oxidized chains. The conduction band gap estimated for **P3OF-95** is 0.34 eV, and that for **P3OF-75** is 0.9 eV. The **P3OF** samples are thermally stable in N_2 atmosphere to between 275 °C (**P3OF-50**) and 380 °C (**P3OF-95**), but suffer thermal oxidation above 150 °C or light-induced oxidation at room temperature.

Introduction

Conjugated polymers have interesting optoelectronic and processing properties that are uniquely suited for a variety of applications, including the active material in thin film transistors (TFTs), light emitting diodes (LEDs), light emitting cells (LECs), electrochromic displays (ECDs), and various NLO applications.[1−5] The *molecular* structural feature responsible for these interesting properties is the system of extended, alternating single and double bonds that gives rise to delocalized π-molecular orbitals (MOs). Simple unsubstituted polymers, e.g. poly(*p*-phenylene) (PPP), poly(phenylenevinylene) (PPV), poly-(thiophene), poly(pyrrole), etc., are extremely insoluble and infusible, and they are therefore difficult or impossible to process into useful forms or devices. These materials are made soluble by the attachment of long alkyl side chains onto the conjugated backbone. However, the alkyl side chains "dilute" the conjugated backbones with the result that the conductivities of the alkyl-substituted polymers are usually orders of magnitude less than that of the insoluble, unsubstituted parent.

Conductivity is a bulk property and, in these conjugated polymers, is best viewed as a charge hopping from molecule to molecule. The conductivity, $\sigma = nq\mu$, is the product of the concentration of charge carriers (n, cm^{-3}), their charge (q, C), and mobility (μ = drift velocity per unit field, $cm^2/V\cdot s$, related to the hopping rate). In pure polymers, the concentration of free carriers is very low because the "band gaps" of these organic materials, mostly determined by the *molecular* HOMO-LUMO gaps, are typically ≥2.5 eV. Conductivities in excess of 10^{-13} S/cm are typically due to inadvertent doping (introduction of charge carriers) by impurities introduced during the synthesis or by contact with atmospheric oxygen.[6] Oxidation or reduction (p-doping and n-doping, respectively) of the neutral polymers raises the carrier concentration to levels approaching the molecular density (ca. $10^{21}/cm^3$). With typical mobilities of 10^{-6} $cm^2/V\cdot s$, the conductivity is then on the order of $\sigma = (10^{21})(10^{-19})(10^{-6}) = 10^{-4}$ S/cm.

Recently, much higher conductivities have been claimed with doped, regioregular thiophenes, i.e., poly(3-alkylthiophene)s (**P3AT**s), whose side chains have a translational symmetry down the polymer backbone.[7,8] Thus, conductivities over 10^3 S/cm have been claimed for head−tail, head−tail (HT-HT) regio-regular **P3AT**s.[7] Such a conductivity implies a carrier mobility

(1) (a) Skotheim, T. A., Ed. *Handbook of Conducting Polymers*; M. Dekker: New York, 1986. (b) Aldissi, M. *Inherently Conducting Polymers*; Noyes Data Corp.: Park Ridge, NJ, 1989. (c) Cotts, D. B.; Reyes, Z. *Electrically Conductive Organic Polymers for Advanced Applications*; Noyes Data Corp.: Park Ridge, NJ, l986. (d) Salaneck, W. R.; Clark, D. T.; Samuelsen, E. J., Eds. *Science and Applications of Conducting Polymers*; IOP Publications Ltd.: Bristol, UK, 1990; p 1.

(2) Roncali, J. *Chem. Rev.* **1992**, *92*, 711−738.

(3) Strukelj, M.; Miller, T. M.; Papadimitrakopoulos, F.; Son, S. *J. Am. Chem. Soc.* **1995**, *117*, 11976.

(4) Holmes, A. B.; Bradley, D. D. C.; Brown, A. R.; Burn, P. L.; Burroughes, J. H.; Friend, R. H.; Grenham, N. C.; Gymer, R. W.; Halliday, D. A.; Jackson, R. W.; Kraft, A.; Martens, J. H. F.; Pichler, K.; Samuel, I. D. W. *Synth. Met.* **1993**, *55*−*57*, 4031.

(5) (a) Horowitz, G. *Adv. Mater.* **1996**, *8*, 177. (b) Lovenger, A. J.; Rothberg, L. J. *J. Mater. Res.* **1996**, *11*, 1581.

(6) Abdou, M. S. A.; Orfino, F. P.; Son, Y.; Holdcroft, S. *J. Am. Chem. Soc.* **1997**, *119*, 4518.

(7) (a) McCullough, R. D.; Tristram-Nagle, S.; Williams, S. P.; Lowe, R. D.; Jayaraman, M. *J. Am. Chem. Soc.* **1993**, *115*, 4910. (b) McCullough, R. D.; Williams, S. P. *J. Am. Chem. Soc.* **1993**, *115*, 11608.

(8) (a) Chen, T.; Wu, X.; Rieke, R. D. *J. Am. Chem. Soc.* **1995**, *117*, 233−244. (b) Wu, X.; Chen, T.; Rieke, R. D. *Macromolecules* **1996**, *29*, 7671. (c) Faid, K.; Frechette, M.; Ranger, M.; Mazerolle, L.; Levesque, I.; Leclerc, M.; Chen, T.; Rieke, R. D. *Chem. Mater.* **1995**, *7*, 1390. (d) Sandstedt, C. A.; Rieke, R. D.; Eckhardt, C. J. *Chem. Mater.* **1995**, *7*, 1057−1059. (e) Chen, T.; Rieke, R. D. *J. Am. Chem. Soc.* **1992**, *114*, 10087.

10.1021/ja003588i CCC: $20.00
Published on Web 02/17/2001

of around 10 $cm^2/V \cdot s$.[9] The higher mobilities are a consequence of the increased order (crystallinity) in the regioregular materials that allows for increased $\pi-\pi$ contact (π-stacking) between neighboring molecules. The better packing in the crystalline regions leads to more planar molecular conformations and shorter intermolecular distances that facilitate carrier hopping from molecule to molecule. The π-stacking distance, determined by X-ray diffraction, is on the order of 3.4−3.6 Å.[7b,11] Similar distances are found in HH-TT regioregular poly(4,4′-dialkyl-2,2′-bithiazoles) [(PABTz)s].[10] Other properties are also affected by π-stacking. The degree of intermolecular electronic interaction is heightened, with the result that optoelectronic properties, e.g. thermochromism[12] and excitonic interactions,[13,14] depend critically on the processing history of the sample.[11,15]

In addition to processing history, intermolecular π-stacking interactions depend critically on the polarity and polarizability of the conjugated backbone, and the polarizability, in turn, is strongly influenced by the nature of the heteroatom in the heterocycle.[16] Stated differently, those properties that are strongly dependent on intermolecular interactions, e.g., conductivity and exciton migration, might respond differently in a poly(furan) compared to the corresponding poly(thiophene). Thus, it is of interest to compare properties of polymers that have similar overall geometries and structures, but differ in the atomic makeup of the main chain.[17] Examples of structurally similar poly(aromatic heterocycles) are poly(dialkylbithiazoles),[10a,15,18] poly(dialkylbisoxazoles),[19] poly(dialkylbithiophenes),[20] and poly(pyrroles), poly(thiophenes), and poly(furans).[21,22] Surprisingly, poly(furans) are among the least well studied of these groups. Prior to the report of Glenis et al., it appears that genuine poly(furan) (PF) had not been prepared.[22] Most previous attempts to prepare PF had been via the oxidative coupling of furan. The high oxidation potentials needed for the coupling also over-oxidized the resulting polymers and led to irreversible degredation. Glenis et al. prepared insoluble films of PF by electrochemical oxidation of ter(furan), the oxidation potential of which is ca. 1.5 V less positive than that of furan. The PF obtained by Glenis et al. possessed the spectral properties expected of the conjugated polymer. However, it is known that the oxidative route, even when successful, often leads to the introduction of defects, e.g., nonconjugated 2,4-coupling, cross-linking, and carbon−halogen bond formation.[23] Such defects can seriously degrade optical and electrical properties. Here, we report the first organometallic synthesis of soluble, processable HT-regioregular and regiorandom poly(alkylfuran) (P3AF), as well as a P3AF with an intermediate degree of regioregularity, and compare the properties of these polymers to those of the better-known poly(3-alkylthiophene)s, **P3AT**s.

Experimental Section

Materials. All manipulations and polymerizations were performed under a nitrogen atmosphere using standard Schlenk line techniques unless otherwise stated. Reagents were purchased and used as received unless otherwise stated. $ZnCl_2$ was dehydrated by refluxing it with thionyl chloride.

X-ray diffraction patterns were obtained on films that were solvent-cast onto thin glass cover slides. Either a Scintag ×1 or a Rigaku Rotoflex powder diffractometer utilizing Cu Ka radiation ($\lambda = 0.154$ nm) was used to collect the diffraction data. ^{1}H NMR spectra were collected on a Bruker AM-360, AM-300, or AM-200 and referenced to the residual proton solvent resonance. UV−vis spectra were collected on a Shimadzu 3101PC with baseline correction. Cyclic Voltammetry (CV) was run using a home-built potentiostat, designed by Wayne Burkhardt, Electronics shop, Department of Chemistry, University of Michigan, interfaced to a PC computer with a custom program written by Dr. S. Paras, Department of Chemistry, University of Michigan. The solvent was dry CH_3CN, and the supporting electrolyte was tetrabutylammonium hexafluorophosphate (0.1 M). The reported potentials are vs the ferrocene/ferrocenium (Fc/Fc^+) couple, obtained by adding a crystal of ferrocene to the solution. The thermal analysis was performed on a Perkin-Elmer DSC/TGA 7. Elemental analyses were performed by either Galbraith Laboratories or the University of Michigan Microanalysis Laboratory. Molecular weight determinations were made by GPC in $CHCl_3$ using a UV detector ($l = 354$ nm) and polystryrene standards.

Theoretical calculations were conducted on a Macintosh computer with the Cache version 4.1 suite of programs. The AM1 method was used to calculate the molecular orbitals and optimize the geometry, and Zindo, using INDO/1 parameters and configuration interaction set to 9 (lowest 81 excited singlet states), was used to calculate the electronic spectra.

Reaction of maleic anhydride with furan (1):[24] A 500 mL round-bottom flask was charged with furan (33.7 g, 0.5 mol) and maleic anhydride (48.5 g, 0.5 mol) in ether (150 mL). The solution was stirred for 24 h during which time a white precipitate formed. The mixture was cooled in a refrigerator and the white crystals were collected. Yield = 60.25 g (70.0%). ^{1}H NMR ($CDCl_3$): δ 3.18 (2H, s), 5.46 (2H, t, $J = 1$ Hz), 6.58 (2H, t, $J = 1$ Hz). MP = 122 °C.

Bromination of 1 (2):[24] A 1 L Schlenk flask equipped with a stir bar and N_2 inlet/outlet was charged with **1** (30.0 g, 0.18 mol) in CH_2Cl_2 (800 mL). Bromine (9.3 mL, 0.18 mol) was added, and the reaction

(9) Intrinsic carrier mobilities may be higher. The measured mobilities include barriers due to grain boundaries, film imperfections, impurity traps, etc.

(10) (a) Nanos, J. I.; Kampf, J. W.; Curtis, M. D.; Gonzalez, L.; Martin, D. C. *Chem. Mater*. **1995**, *7*, 2232. (b) Gonzales Ronda, L.; Martin, D. C.; Nanos, J. I.; Politis, J. K.; Curtis, M. D. *Macromolecules* **1999**, *32*, 4558.

(11) (a) Yang, C.; Orfino, F. P.; Holdcroft, S. *Macromolecules* **1996**, *29*, 6510. (b) Park, K. C.; Levon, K. *Macromolecules* **1997**, *30*, 3175. (c) Prosa, T. J.; Winokur, M. J.; McCullough, R. D. *Macromolecules* **1996**, *29*, 3654.

(12) (a) Inganäs, O. *Trends Polym. Sci.* **1994**, *2*, 189−196. (b) Roux, C.; Leclerc, M. *Chem. Mater.* **1994**, *6*, 620. (c) Leclerc, M.; Faid, K. *Adv. Mater.* **1997**, *9*, 1087. (d) Dufresne, G.; Bonchard, J.; Beletête, M.; Durocher, G.; Leclerc, M. *Macromolecules* **2000**, *33*, 8252.

(13) Koren, A. B.; Curtis, M. D.; Kampf, J. W. *Chem. Mater.* **2000**, *12*, 1519.

(14) (a) Yamamoto, T.; Komarudin, D.; Arai, M.; Lee, B.; Suganuma, H.; Asakawa, N.; Inoue, Y.; Kubota, K.; Sasaki, S.; Fukuda, T.; Matsuda, H. *J. Am. Chem. Soc*. **1998**, *120*, 2047. (b) Halkyard, C. E.; Rampey, M. E.; Kloppenburg, L.; Studer-Martinez, S. L.; Bunz, U. H. F. *Macromolecules* **1998**, *31*, 8655. (c) Langeveld-Voss, B. M. W.; Janssen, R. A. J.; Christiaans, M. P. T.; Meskers, S. C. J.; Dekkers, H. P. J. M.; Meijer, E. W. *J. Am. Chem. Soc.* **1996**, *118*, 4908. (d) Langeveld-Voss, B. M. W.; Waterval, R. J. M.; Janssen, R. A. J.; Meijer, E. W. *Macromolecules* **1999**, *32*, 227.

(15) (a) Yamamoto, T.; Suganuma, H.; Maruyama, T.; Inoue, T.; Muramatsu, Y.; Arai, M.; Komarudin, D.; Ooba, N.; Tomaru, S.; Sasaki, S.; Kubota, K. *Chem. Mater.* **1997**, *9*, 1217.

(16) (a) Saadeh, H.; Goodson, T.; Yu, L. *Macromolecules* **1997**, *30*, 4608. (b) Burke, L. A.; Kao, J.; Lilly, A. C. *J. Comput. Chem.* **1987**, *8*, 107−16.

(17) Yang, C.; Abley, M.; Holdcroft, S *Macromolecules* **1999**, *32*, 6889.

(18) Politis, J. K.; Curtis, M. D.; González L.; Martin, D. C.; He, Y. *Chem. Mater*. **1998**, *10*, 1713.

(19) (a) Politis, J. K.; Curtis, M. D.; González-Ronda, L.; Martin, D. C. *Chem. Mater*. **2000**, *12*, 2798. (b) Politis, J. K.; Somaoza, F. B.; Kampf, J. W.; Curtis, M. D.; González-Ronda, L.; Martin, D. C. *Chem. Mater*. **1999**, *11*, 2274.

(20) (a) Roux, C.; Bergeron. J.-Y.; Leclerc, M. *Makromol. Chem*. **1993**, *194*, 869. (b) Faïd, K.; Cloutier, R.; Leclerc, M. *Macromolecules* **1993**, *26*, 2501.

(21) (a) Ohsawa, T.; Kaneto, K.; Yoshino, K. *Jpn. J. Appl. Phys.* **1984**, *23*, L663. (b) Benvenuti, F.; Galletti, A. M.; Carlin, C.; Sbrana, G.; Nannini, A.; Bruschi, B. *Polymer* **1997**, *38*, 4973. (c) Nishioka, Y.; Wang, S.; Yoshino, K. *Synth. Met.* **1991**, *41*−*43*, 815. (d) Zotti, G.; Schiavon, G.; Comisso, N.; Berlin, A.; Pagani, G. *Synth. Met.* **1990**, *36*, 337.

(22) Glenis, S.; Benz, M.; LeGoff, E.; Schindler, J. L.; Kannewurf, C. R.; Kanatzidis, M. G. *J. Am. Chem. Soc*. **1993**, *115*, 12519.

(23) (a) Abdou, M. S. A.; Lu, X.; Xie, Z. W.; Orfino, F.; Deen, M. J.; Holdcroft, S. *Chem. Mater*. **1995**, *7*, 631. (b) Souto Maior, R. M.; Hinkelmann, K.; Eckert, H.; Wudl, F. *Macromolecules* **1990**, *23*, 1268. (c) Krishe, B.; Zagorska, M. *Synth. Met.* **1989**, *28*, C263.

(24) (a) Berson, J. A.; Swidler, R. *J. Chem. Soc.* **1953**, *75*, 1721. (b) Berson, J. A.; Swidler, R. *J. Chem. Soc.* **1954**, *78*, 4060.

mixture was allowed to stir for 3.5 h. The slightly yellow mixture was filtered, and the solid was washed with CH_2Cl_2 to give a white solid. The CH_2Cl_2 washings were concentrated to give a white crystalline solid. Both solids were washed separately with ether and collected. MS ($M^+ = 325$) indicated both solids were product. Yield: 47.95 g (81.7%). ^{1}H NMR ($(CD_3)_2CO$): δ 4.04 (2H, dd, $J_A = 39.5$ Hz, $J_B = 6.8$ Hz), 4.45 (1H, d, $J = 3.3$ Hz), 4.58 (1H, t, $J = 4.0$ Hz), 5.05 (1H, s), 5.25 (1H, d, $J = 4.9$ Hz).

Synthesis of 3-bromofuran:[25] A 250 mL round-bottom flask equipped with a stir bar and a short path distillation head, with the collection flask emersed in a dry ice/acetone bath, was charged with **2** (26.31 g, 80.7 mmol) in quinoline (20 mL) and the mixture was heated. A slightly colored liquid was distilled between 50 and 140 °C. GC-MS showed the presence of both the desired product and quinoline. ^{1}H NMR also showed the presence of furan. The liquid was distilled in air to give the product (bp = 104 °C). Yield 4.04 g (34%). ^{1}H NMR ($CDCl_3$): δ 6.45 (1H, dd, $J_A = 0.76$ Hz, $J_B = 1.9$ Hz), 7.37 (1H, t, $J = 1.8$ Hz), 7.44 (1H, dd, $J_A = 0.84$ Hz, $J_B = 1.6$ Hz). GC-MS: 1 peak, $M^+ = 148$.

Synthesis of 3-octylfuran:[26] A 100 mL round-bottom three-neck flask equipped with a stir bar, condenser, addition funnel, and N_2 inlet/outlet was charged with Mg (0.79 g, 32.7 mmol) in dry ether (10 mL). Bromooctane (6.31 g, 32.7 mmol) in dry ether (20 mL) was added dropwise to maintain a mild reflux. The mixture was refluxed for an additional 2.5 h. The Grignard reagent solution was added dropwise to a 250 mL three-neck, round-bottom flask containing 3-bromofuran (4.00 g, 27.2 mmol) and Ni(dppp)Cl_2 (0.44 g, 0.82 mmol) in dry ether (30 mL) at 0 °C. The solution was allowed to reflux overnight. The reaction mixture was quenched carefully with HCl (5%, 75 mL), and the ether layer was washed with H_2O (2 × 75 mL) and dried over $MgSO_4$. The ether was evaporated (Rotovap) to give a liquid that was distilled under vacuum (~0.05 Torr). The product, collected between 40 and 45 °C, was a clear liquid. Yield = 0.87 g (17.7%). ^{1}H NMR ($CDCl_3$): δ 0.88 (3H, t, $J = 6.5$ Hz, $-CH_3$), 1.20−1.45 (12H, m, $-(CH_2)_6CH_3$), 1.51 (2H, m, $J = 6.9$ Hz, ring-CH_2CH_2), 2.40 (2H, t, $J = 7.4$ Hz, ring-CH_2), 6.27 (1H, t, $J = 0.75$ Hz, 3-position ring proton), 7.20 (1H, m, $J = 0.93$ Hz, ring proton), 7.34 (1H, t, $J = 1.66$ Hz, ring proton). UV−vis ($CHCl_3$): 244 nm. GC-MS shows 1 peak: $M^+ = 180$.

Synthesis of 2,5-dibromo-3-octylfuran (3): A 100 mL Schlenk flask equipped with a stir bar, addition funnel, and N_2 inlet/outlet was charged with 3-octylfuran (0.48 g, 2.66 mmol) in hexanes (10 mL). The solution was cooled to 0 °C and covered with Al foil, and bromine (0.85 g, 5.32 mmol) in hexanes (15 mL) was added dropwise. The solution was stirred at 0 °C for 2 h during which time the reaction loses some color. The mixture was allowed to stir at room temperature for an additional 2 h. The light yellow solution was washed with $NaHCO_3$ (saturated, 2 × 50 mL) and $NaHSO_3$ (saturated, 50 mL) and dried over $MgSO_4$. The solvent was removed to give a slightly yellow liquid. Yield = 0.67 g (74.5%). ^{1}H NMR ($CDCl_3$): δ 0.88 (3H, t, $J = 6.4$ Hz, $-CH_3$), 1.20−1.40 (12H, m, $-(CH_2)_6CH_3$), 1.49 (2H, m, $J = 6.6$ Hz, ring-CH_2CH_2), 2.31 (2H, t, $J = 7.4$ Hz, ring-CH_2), 6.22 (1H, s, 3-position ring proton). MS(EI): $M^+ = 338$.

Synthesis of HT-regioregular poly(3-octylfuran), P3OF-95: 2,5-Dibromo-3-octylfuran (2.21 g, 6.55 mmol) in dry THF (13 mL) was added via cannula to a 100 mL Schlenk flask containing freshly prepared Zn[8a] (7.58 mmol) in THF (25 mL) at −78 °C. The mixture was stirred at −78 °C for 1 h and allowed to warm to 0 °C over 3 h. Ni(dppe)$_2Cl_2$ (7 mg, 0.013 mmol) in dry THF (13 mL)was added via cannula at 0 °C and the dark mixture was allowed to stir for 24 h. The reaction mixture was poured into MeOH and the red precipitate was collected. The solid was reprecipitated twice from $CHCl_3$ into MeOH to give a dark red polymer with a metallic, green tint. Yield = 0.80 g (67.9%). ^{1}H NMR ($CDCl_3$): δ 0.79−1.10 (3H, $-CH_3$), 1.12−1.63 (10 H, $-(CH_2)_5CH_3$), 1.64−1.80 (2H, ring-CH_2CH_2), 2.65−2.95 (2H, ring-CH_2), 6.40−6.65 (1H, ring proton). λ_{max} (abs) = 466, 493, 537 nm (soln). λ_{max} (abs) = 466, 493, 537 nm (film). MW: $M_n = 75$kD, $M_w = 213$kD.

(25) Srogi, J.; Janda, M.; Stibor, I. *Collect. Czech. Chem. Commun.* **1970**, *35*, 3478.

(26) Van Pham, C.; Mark, H. B.; Hans Zimmer, H. *Synth. Commun.* **1986**, *16*, 689.

Scheme 1

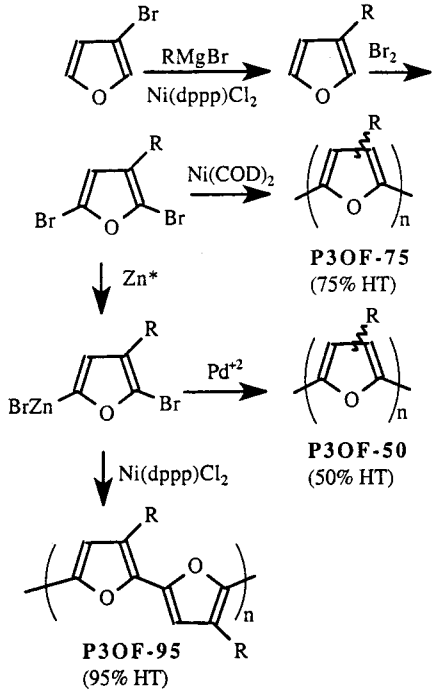

Synthesis of regiorandom poly(3-octylfuran), P3OF-50: 2,5-Dibromo-3-octylfuran (2.37 g, 7.0 mmol) in dry THF (14) was added to a 100 mL Schlenk flask containing freshly prepared Reike Zn[8a] in THF (28 mL) via cannula at 0 °C. The mixture was stirred at room temperature for 1 h and Pd(PPh_3)$_4$ (24 mg, 0.021 mmol) in THF (14 mL) was added. The dark mixture was stirred at room temperature for 24 h and poured into MeOH. The mixture was filtered through a 1/4 in. plug of Celite and the polymer was extracted from the Celite with $CHCl_3$. The solvent volume was reduced and the polymer was reprecipitated into MeOH. The polymer was collected on a 1/4 in. plug of Celite and extracted with $CHCl_3$. The $CHCl_3$ was removed in vacuo to give a red paste. Yield = 0.50 g (39.7%). ^{1}H NMR ($CDCl_3$): δ 0.79−1.10 (3H, $-CH_3$), 1.12−1.63 (10 H, $-(CH_2)_5CH_3$), 1.64−1.80 (2H, ring-CH_2CH_2), 2.30−2.50 (1H from HH coupling, ring-CH_2), 2.65−2.95 (1H from HT coupling, ring-CH_2), 6.35−6.65 (1H, ring proton). λ_{max}(abs) = 372 nm (soln). λ_{max}(abs) = 382 nm (film). MW: $M_n = 7400$, $M_w = 93$kD.

Synthesis of partially regioregular poly(3-octylfuran), P3OF-75. Ni(cod)$_2$ (2.66 g, 9.41 mmol) and 2,2′-bipyridine (1.51 g, 9.64 mmol) in dry toluene (100 mL) were added to a 100 mL Schlenk flask. The dark purple solution was then added to 2,5-dibromo-3-octylfuran (2.65 g, 7.8 mmol) in a 250 mL three-neck flask. The dark mixture was heated for 20 h, then cooled and filtered through Celite. The Celite was rinsed with $CHCl_3$ until the filtrate was colorless. The filtrate volume was reduced, and the product was then precipitated by pouring the solution into stirred MeOH. The suspension was filtered through a 1/4 in. plug of Celite, and the polymer was extracted from the Celite with $CHCl_3$. The filtrate volume was again reduced, and the polymer was reprecipitated into MeOH. The polymer was then collected by filtration and dried under vacuum to yield a dark red, rubbery polymer. Yield = 0.97 g (69.9%). ^{1}H NMR ($CDCl_3$): δ 0.79−0.97 (3H, $-CH_3$), 1.00−1.55 (10 H, $-(CH_2)_5CH_3$), 1.60−1.80 (2H, ring-CH_2CH_2), 2.20−2.50 (0.48H from HH coupling, ring-CH_2), 2.65−2.95 (1.52H from HT coupling, ring-CH_2), 6.30−6.70 (1H, ring proton). λ_{max} (abs) = 437 nm (soln). λ_{max} (abs) = 452 nm (film). MW: $M_n = 49$kD, $M_w = 93$kD.

Results and Discussion

Preparation. Scheme 1 shows the synthetic route employed. The starting point for **P3AT** synthesis is 3-bromothiophene, prepared by tribromination of thiophene and then removal of the more reactive bromine atoms at the 2,5-positions. A similar

Scheme 2

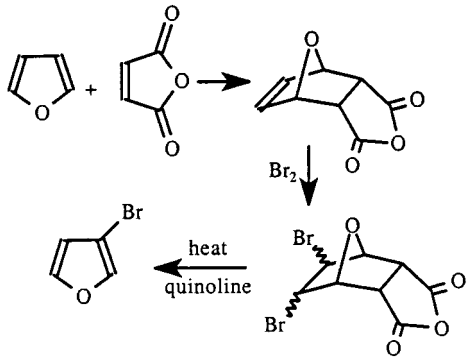

route to 3-bromofuran was ineffectual. Attempts at tribromination of furan gave complex mixtures of products. Tribromofuran could be isolated from these mixtures in low yield, but the product appeared to be thermally and photolytically unstable. The desired 3-bromofuran was prepared as shown in Scheme 2 by first making the Diels−Alder (D−A) adduct of furan with maleic anhydride. The D−A adduct was brominated and then subjected to a simultaneous dehydrobromination/retro-Diels−Alder reaction by heating it in quinoline. The 3-bromofuran was obtained in 50% yield from the D−A adduct. Octylmagnesium bromide was coupled to the 3-bromofuran with Ni(dppp)Cl_2 catalyst in 18% yield. Bromination of the octylfuran gave 2,5-dibromo-3-octylfuran in 74% yield.

The synthesis of regioregular- and regiorandom-**P3OF** is strictly analogous to the Rieke method of preparing the corresponding **P3AT**s. This method entails the formation of 2-bromo-5-bromozincio-3-octylfuran by the reaction of the dibromide with activated (Rieke) zinc. The regioselectivity of this zincation reaction is not crucial because the catalysts used for the coupling reaction also catalyze the scrambling of the C−Br and C−Zn bonds. The critical regioselectivity presumably occurs during the reductive elimination of the new C−C bond: the Ni(II) catalyst produces regioregular HT-HT coupling, whereas the Pd(0) catalyst leads to completely random HT-, HH-, and TT-coupled product. The behavior of 2,5-dibromo-3-octylfuran mirrored that of the thiophenes: the Ni(II) catalyst gave a dark red polymer (M_n = 75 000, PDI = 2.84), films of which exhibit a metallic green, specular reflection, whereas the Pd catalyst gave a red, pasty low MW polymer (M_n = 7400, PDI = 12.6). A third preparative method utilized direct coupling of 2,5-dibromo-3-octylfuran with bis(cyclooctadiene)nickel(0), Ni(cod)$_2$. This method gave a rubbery, red polymer (M_n = 49 000, PDI = 1.9), with an intermediate degree of HT-coupling as described below.

Figure 1 shows the α-methylene and aromatic regions of the ^{1}H NMR spectra of **P3OF** prepared by the first two methods. The α-methylene protons are sensitive to the diad structure and have equal probability of being in a HH or a HT environment in a completely regiorandom polymer. The HT-α-methylene signal occurs at 2.81 ppm, and the HH peak appears at 2.36 ppm. The relative area ratio of the two peaks can be used to determine the regioregularity. The HT:HH ratio of the polymer prepared by the Rieke method with the Ni catalyst was 19:1, indicating 95% regioregular HT coupling, whereas the polymer prepared from the Pd catalyst was regiorandom as evidenced by the 1:1 ratio of the two α-methylene peaks. The α-methylene ratio of the polymer made from Ni(cod)$_2$ coupling was 3:1, corresponding to a 75% regioregular HT content. The NMR spectrum in the ring proton region confirms this assignment. The resonance frequency of the ring protons is sensitive to the

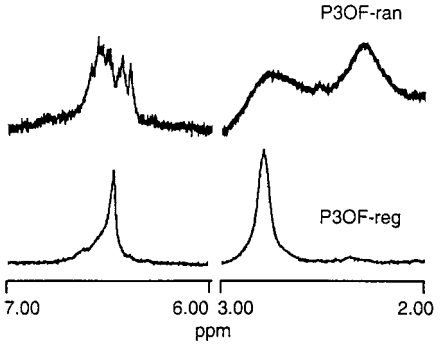

Figure 1. The α-methylene and aromatic regions in the NMR spectra of **P3OF-50** (ran) and **P3OF-95** (reg).

Scheme 3

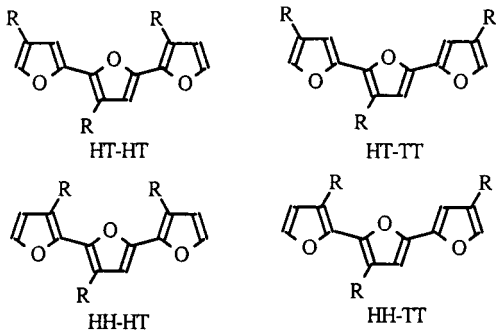

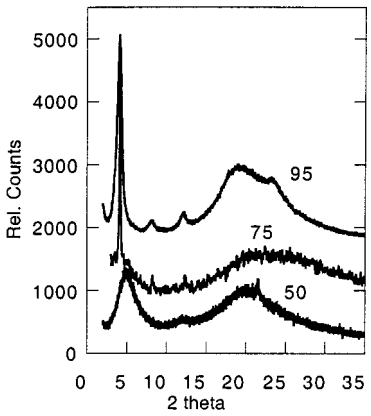

Figure 2. XRD patterns of solid films of **P3OF-95**, **-75**, and **-50.**

triad structure. In a regiorandom polymer, the four triads shown in Scheme 3 are equally probable, so the signals of the ring protons appear as four equally intense peaks in a random polymer. Only a single ring-proton environment exists in the HT-regioregular material. In the regioregular polymer prepared with the Ni(II) catalyst in the Rieke method, only one ring proton signal is seen at 6.47 ppm, but the polymers from the Rieke method with Pd catalyst and from the coupling with Ni(cod)$_2$ showed at least three peaks between 6.35 and 6.65 ppm (one of which is broad and is probably unresolved). The regioregular, regiorandom, and intermediate **P3OF** polymers will be denoted by the percentage of HT-links in the sample: **P3OF-95**, **P3OF-50**, and **P3OF-75**, respectively.

X-ray Diffraction. Figure 2 shows an overlay of the XRD patterns of the three poly(octylfuran)s. **P3OF-95** shows strong first, second, and third order diffraction peaks at 2θ of 4.0°, 8.0°, and 12.1° which correspond to d-spacings of 22.1, 11.1, and 7.2 Å, respectively. These peaks are assigned to the (100), (200), and (300) reflections, respectively. Another diffraction peak, centered at 2θ = 23.3°, corresponds to d-spacing of 3.81 Å. **P3OF-50** has a broad diffraction peak at 2θ = 4.5° that

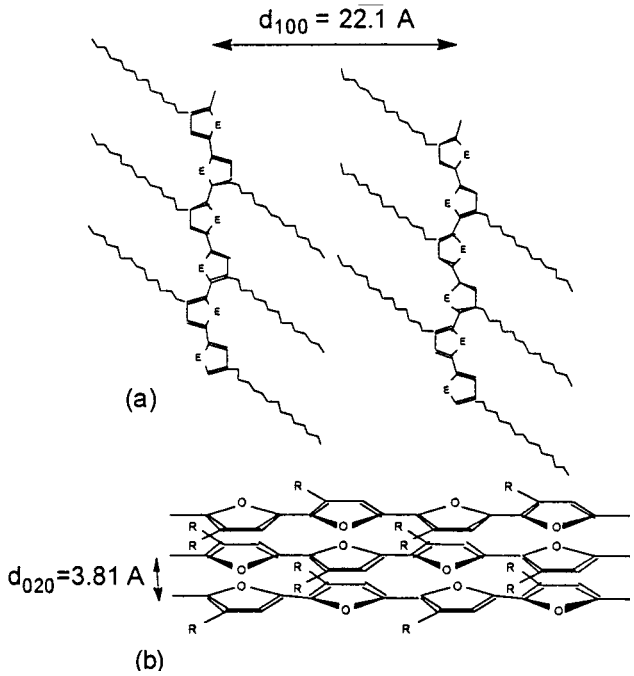

Figure 3. Idealized spacing of (a) lamellae and (b) π-stacking in **P3OF-95**.

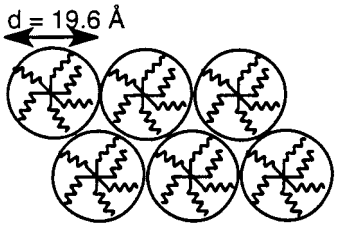

Figure 4. Possible solid-state conformation of **P3OF-50** (looking down the chain axis).

corresponds to a d-spacing of 19.6 Å. The d-spacing of 22.1 Å in **P3OF-95** is assigned to the d_{100} lamellar spacing between the polymer chains, and the d-spacing of 3.81 Å is assigned to d_{020} and corresponds to the interchain, π-stacking distance. Both distances are illustrated in Figure 3. The shorter d-spacing, 19.6 Å, in **P3OF-50** arises from disorder in the alkyl chain conformations and twist defects in the conjugated backbone as illustrated in the along-the-chain projection in Figure 4. This interpretation of the XRD data is identical to that proposed for poly(nonylbithiazole) (**PNBTz**), in which both crystalline and amorphous forms were isolated and analyzed by XRD.[10] It was shown that the amorphous, yellow **PNBTz** film has a d-spacing of 20.1 Å and the crystalline red film has a $d_{100} = 24.5$ Å. The XRD of **P3OF-75** has a large amorphous region but shows the d_{100} and higher order peaks found in the more crystalline regioregular polymer.

A comparison of the XRD data of the analogous thiophene polymer, **HT-P3OT**, with that of **P3OF-95** reveals that the two structures are very similar. The lamellar spacing in **HT-P3OT** is 20.2 Å,[11] slightly shorter than the 22.1 Å in **P3OF-95**. The π-stacking distances are nearly identical: 3.79 Å vs 3.81 Å. The larger distances in the poly(furan) structure are a bit surprising. The π-stacked polymer chains are typically "slipped" with respect to neighboring chains by one ring distance, i.e., the crystallographic repeat distance perpendicular to the chain backbone is twice the distance between neighboring chains.[10,11] This "slippage" places the sulfur (or oxygen) atoms in the rings of one chain into close proximity with the 3,4-carbon atoms in

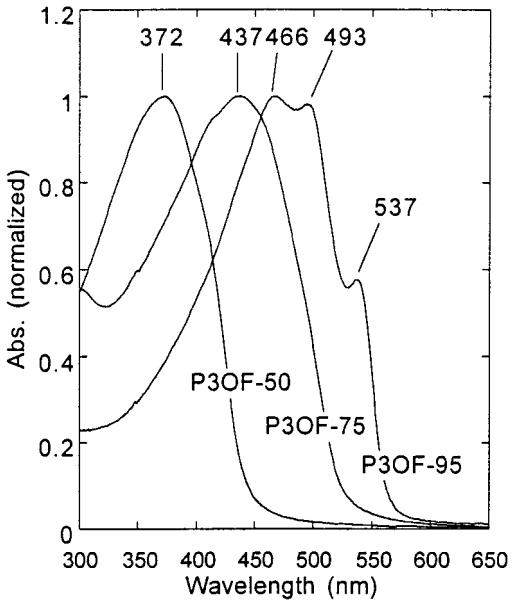

Figure 5. UV−vis absorption spectra of **P3OF-50**, **-75**, and **-95** in solution.

the rings on neighboring chains. Since the van der Waals radius of sulfur is greater than that of oxygen, one would expect the thiophenes to have a larger π-stacking (d_{020}) distance, but this is not observed experimentally. Perhaps the higher polarizability of sulfur vs oxygen produces greater interchain van der Waal attractions in **P3OT** vs **P3OF**, leading to a smaller than expected π-stacking distance in the former. Alternatively, the rings may also stack with some slippage sidewise to the chain direction. A slight side-slippage increases the interchain interatomic distances but does not increase the interplanar spacing. It may be noted that a similar oxygen-for-sulfur substitution that converts poly(nonylbithiazole) (**PNBTz**) to poly(nonylbisoxazole) (**PNBO**) has been made, and the π-stacking distance in **PNBTz** is, as expected, larger than that of **PNBO** (3.59 vs 3.30 Å).[19] The differences in the lamellar spacing (d_{100}) can be related to different angles subtended by the side chain with respect to the main chain. Experimentally, different angles have been observed in the solid-state structures of bithiophenes, bithiazole, and bisoxazole oligomers.[19]

UV−Vis Spectroscopy. Figures 5 and 6 show the UV−vis spectra of solutions and solid films, respectively, of the three poly(octylfuran)s prepared in this work. **P3OF-95** has three absorption peaks in both solution and the solid state. In solution, two intense peaks are observed at 466 and 493 nm with a shoulder at 537 nm, whereas in the solid state, the 466 nm peak becomes a shoulder, and the 537 nm feature becomes sharper and more prominent. **P3OF-50** has a single absorption peak at 372 nm in solution that broadens and shifts to 386 nm in the solid. The spectra of **P3OF-75** showed intermediate character: a single absorption peak at 437 nm in solution that shifts to 452 nm in the film.

The absorption maxima, λ_{max}, of conjugated polymers commonly show a red shift in the solid state as compared to the solution. This shift can range from as little as a few nm to around 100 nm and depends on the relative conformations of the polymer chains in the solution and solid-state phases. If the polymer backbone is twisted so that the rings comprising the main chain are not coplanar, then the effective conjugation is decreased, the HOMO-LUMO gap is increased, and the polymer absorbs at shorter wavelengths.[8,10−12] Alkyl-substituted aromatic or heteroaromatic polymers tend to crystallize in the π-stacked,

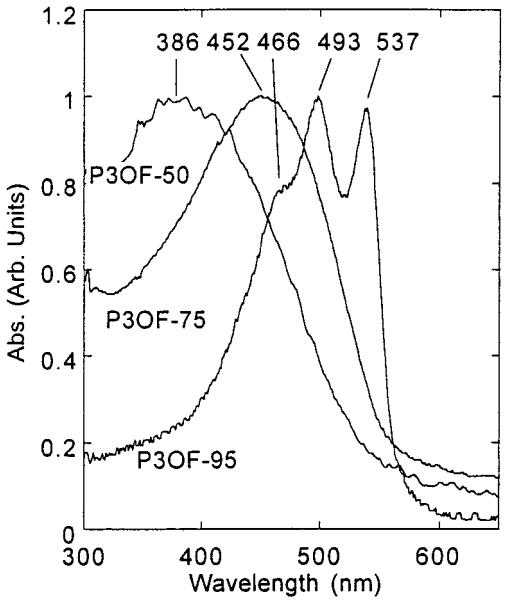

Figure 6. UV−vis absorption spectra of **P3OF-50**, **-75**, and **-95** cast in thin solid films.

lamellar structure discussed above, with the consequence that the main chain adopts a planar conformation with an increased effective conjugation length and longer wavelength absorption.[27] Bulky groups on the side chain inhibit π-stacking, such that the absorption maxima of the solution and solid essentially overlap.[18] Hence, the short wavelength absorption and the relatively small (14 nm) red shift from solution to solid state in λ_{max} of **P3OF-50** are indicative of disorder and nonplanar backbones in both phases. In the more regular **P3OF-75**, the λ_{max} is red shifted relative to **P3OF-50** by about 65 nm in both solution and solid film. This indicates that there are more planar segments in **P3OF-75** than in the random polymer. However, as with **P3OF-50**, there is only a small shift (15 nm) between the solution and solid state, showing that the average chain conformation does not change appreciably as **P3OF-75** solidifies. These conclusions are corroborated by the XRD graphs in Figure 2. **P3OF-50** is essentially amorphous. **P3OF-75** shows some lamellar structure, but no peak near $2\theta = 25°$, characteristic of π-stacked, planar main chains, is observed.

The spectra of **P3OF-95** show long wavelength shoulders or multiple peaks, and very little shift in absorbance maxima between the solution and solid state, showing again that the average chain conformations in solution and solid are nearly identical. In this case, however, the long wavelengths of absorption, the presence of multiple peaks, and the observation of the π-stacking peak in the XRD at 23° all indicate the presence of planar main chains. DuFresne et al. have found recently that phenylene−furanylene copolymers are more rigid (planar) than their thiophene counterparts, and these furan-based polymers also have essentially the same conformations in solution and in solid films.[12d] Yamamoto et al. have convincingly shown that the fine structure observed on the principal UV−vis absorption peak of **HT-P3AT**s in "solution" is associated with the formation of colloidal aggregates.[14a] The colloidal particles have molecular packing that is nearly the same as that in the solid, so that the exciton band structures, etc., are very similar in the two phases.[14,28] It is interesting to note that MeOH (a poor solvent) must be added to $CHCl_3$ solutions of **P3OT** or **PNBTz** to induce aggregation.[14a] However, the more polar and more rigid[12d] oxygen analogues, **P3OF** and **PNBO**,[19] are less soluble, and both exhibit aggregation behavior even in "good" solvents, e.g., $CHCl_3$ or dichloroethane.

The origin of the multiple peaks or "fine structure" on the main $\pi-\pi^*$ absorption peak is still a matter of some debate.[13,19a,29] These peaks are only observed in regioregular, conjugated polymers in the solid state (or in colloidal aggregates that have molecular packing similar to that of the semicrystalline solids), and then only when the size of the side chains allows for close approach of the π-systems on neighboring chains (π-stacking).[18,30,31] The cause of the multiple peaks has been ascribed to absorption of polymer segments with different, yet discrete, effective conjugation lengths,[8a,d,32] to vibronic coupling,[33] and, more recently, to Davydov splitting of the exciton levels by inequivalent sites in the solid,[14b,28,34,35] or to combinations of Davydov splitting and the effects of exciton band density-of-state structure.[13] It is extremely unlikely that the peaks arise from chain segments with different conjugation lengths because the spectra of monodisperse, short-chain, crystalline, conjugated oligomers often show fine structure that is almost identical in form to that in Figure 6.[13,30,31] In these crystalline oligomers, all the molecules are planar, and all have the same conjugation length.

The *purely* vibronic mechanism for producing the fine structure also has some problems, at least in explaining the spectra of polymers that do not contain vinylene groups. The relative intensities of the fine structure shown in Figures 5 and 6 are not characteristic of typical Franck−Condon vibronic envelopes, and there is not a progression of equally spaced peaks commonly seen in systems with strong coupling to only a few vibrations.[31a−b,36] The $\pi-\pi^*$ transition dipole lies in the plane of the ring, and so the $\pi-\pi^*$ transition couples strongly with

(27) (a) Liao, J.-H.; Benz, M.; LeGoff, E.; Kanatzidis, M. G. *Adv. Mater.* **1994**, *6*, 135. (b) Meille, S. V.; Farina, A.; Bezziccheri, F.; Gallazzi, M. C. *Adv. Mater.* **1994**, *6*, 848.

(28) (a) Spano, F. C.; Siddiqui, S. *Chem. Phys. Lett.* **1999**, *314*, 481. (b) DiCésare, N.; Belletête, M.; Leclerc, M.; Durocher, G. *Chem. Phys. Lett.* **1998**, *291*, 487. (c) Chen, L. H.; Geiger, C.; Perlstein, J.; Whitten, D. G. *J. Phys. Chem. B* **1999**, *103*, 9161. (d) Langeveld-Voss, B. M. W.; Waterval, R. J. M.; Janssen, R. A. J.; Meijer, E. W. *Macromolecules* **1999**, *32*, 227.

(29) Miteva, T.; Palmer, L.; Kloppenburg, L.; Neher, D.; Bunz, U. H. F. *Macromolecules* **2000**, *33*, 652.

(30) Curtis, M. D.; Blanda, W.; Politis, J. K.; Francis, A. H.; Lee, J.; Koren, A.; Kampf, J. W.; Gonzalez-Ronda, L.; Martin, D. C. *Mater. Res. Soc. Symp. Proc.* **1999**, 548 (Solid State Ionics), 285.

(31) (a) Cornil, J.; Beljonne, D.; Heller, C. M.; Campbell, I. H.; Laurich, B. K.; Smith, D. L.; Bradley, D. D. C.; Müllen, K.; Brédas, J. L. *Chem. Phys. Lett.* **1997**, *278*, 139. (b) Cornil, J.; Beljonne, D.; Shuai, Z.; Hagler, T. W.; Campbell, I.; Bradley, D. D. C.; Brédas, J. L.; Spangler, C. W.; Müllen, K. *Chem. Phys. Lett.* **1995**, *247*, 425. (c) Shuai, Z.; Brédas, J. L.; Su, W. P. *Chem. Phys. Lett.* **1994**, *228*, 301. (d) Curtis, M. D. In *Photoinduced Charge Transfer*; Rothberg, L., Ed.; World Scientific: Singapore, 2000; pp 77−91.

(32) McCullough, R. D.; Ewbank, P. C. In *Handbook of Conducting Polymers*; Skotheim, T. A., Elsenbaumer, R. L., Reynolds, J. R., Eds.; Mercel Dekker: New York, 1998; pp 243−247.

(33) (a) Sakurai, K.; Tachibana, H.; Shiga, N.; Terakura, C.; Matsumoto, M.; Tokura, Y. *Phys. Rev. B* **1997**, *56*, 9552. (b) Danno, T.; Kuerti, J.; Kuzmany, H. *Frontiers in Polymer Research [Proceedings of the International Conference on Frontiers of Polymer Research]*, 1st; Prasad, P. N., Nigam, J. K., Eds.; Plenum: New York, 1991; pp 219−222. (c) Yamamato, T.; Honda, K.; Ooba, N.; Tomaro, S. *Macromolecules* **1998**, *31*, 7.

(34) (a) DiCesare, N.; Belletete, M.; Marrano, C.; Leclerc, M.; Durocher, G. *J. Phys. Chem.* **1999**, *103*, 795. (b) DiCesare, N.; Belletete, M.; Leclerc, M.; Durocher, G. *J. Phys. Chem.* **1999**, *103*, 803. (c) DiCesare, N.; Belletete, M.; Garcia, E. R.; Leclerc, M.; Durocher, G. *J. Phys. Chem.* **1999**, *103*, 3864.

(35) (a) Beljonne, D.; Langeveld-Voss, B. M. W.; Shuai, Z.; Janssen, R. A. J.; Meskers, S. C. J.; Meijer, E. W.; Bredas, J. L. *Synth. Met.* **1999**, *102*, 912. (b) Bosisio, R.; Botta, C.; Colombo, A.; Destri, S.; Porzio, W.; Grilli, E.; Tubino, R.; Bongiovanni, G.; Mura, A.; DiSilvestro, G. *Synth. Met.* **1997**, *87*, 23.

(36) Broude, V. L.; Rashba, E. I.; Sheka, E. F. *Spectroscopy of Molecular Excitons*; Springer Ser. Chem. Phys. 16; Goldanskii, V. I., Ed.; Springer-Verlag: Duesseldorf, Germany, 1985.

only one or two totally symmetric, in-plane vibrations, e.g., C=C or C=N ring stretches. These are in the region 1450−1515 cm^{-1} in five-membered heterocycles.[34b,37] The separations between the three peaks in the spectrum of **P3OF-95** are 1086 and 1664 cm^{-1} (the peak positions are 21370, 20284, and 18620 cm^{-1}). The latter separation is probably too large to be attributed to a totally symmetric ring mode. The mismatch between the UV−vis peak separations and the frequency of the ring modes is especially evident in the case of **PNBO**: the separation between the two lowest energy peaks is 1780 cm^{-1}, larger than any of the ring vibrations, symmetric or asymmetric.[19] Cornil et al.[31a,b] have successfully fit the fine structure observed on the absorption and emission spectra of PPV derivatives with the use of two vibrational frequencies: 1326 and 1670 cm^{-1}. The latter frequency is most likely associated with the relatively weakly coupled stretching vibration of the vinylene group since polymers, e.g., **P3AT**s or **P3OF**, that do not contain the vinylene group do not display this high-frequency mode.

Furthermore, it is hard to understand why there is strong vibronic coupling in **P3OF-95** whereas none is observed in **P3OF-50**. The coupling between the delocalized electronic excitation and the localized vibrational modes decreases as the electronic excitation is spread over more rings, i.e., the longer the effective conjugation length, the weaker the vibronic coupling.[31b,c] By this argument, **P3OF-95** should have less vibronic structure than **P3OF-50**. The lack of observable vibronic coupling in more regiorandom polymers, e.g., **P3OF-50**, has been ascribed to inhomogeneous broadening of the spectra in the "more heterogeneous" polymers with low HT content. However, this intuitively appealing argument needs further investigation. The sequence length distributions (SLDs) of HT-coupled rings in **P3AT**s and related polymers has been calculated and the spectral line shape (sans vibronic coupling) for the $\pi-\pi^*$ transition simulated as a function of HT content.[38] Polymers with lower HT content have a *narrow* distribution of HT-sequence lengths, dominated by runs of 2−3 rings that are HT coupled before the run is interrupted by a HH or TT coupling. The regioregular polymers, on the other hand, have a very flat and broad distribution of sequence lengths, i.e., the regular polymers contain *all* the sequence lengths, from very short to very long, in comparable amounts. If HH couplings disrupt and shorten the effective conjugation length of a polymer segment, then the regioregular polymers are more "heterogeneous" in terms of distributions of effective conjugation lengths. However, the frequencies of the $\pi-\pi^*$ transitions from the longer sequence lengths overlap because the transition energies are proportional to the *reciprocal* of the conjugation lengths. Thus, the low energy transitions "pile up" and produce a narrow peak with a steeply rising low energy edge while the short conjugation segments produce the long, high energy "foot" (cf. Figure 6). The few short sequence lengths in the regiorandom polymers have relatively widely separated $\pi-\pi^*$ transition energies, and these peaks overlap to give a broader peak with a more gently sloping low energy edge that may obscure the vibronic fine structure.[38]

The fine structure must be associated with the solid-state morphology of the materials: if the XRD peak due to π-stacking is not present, then neither is the typical UV absorption fine structure. We have recently demonstrated that essentially

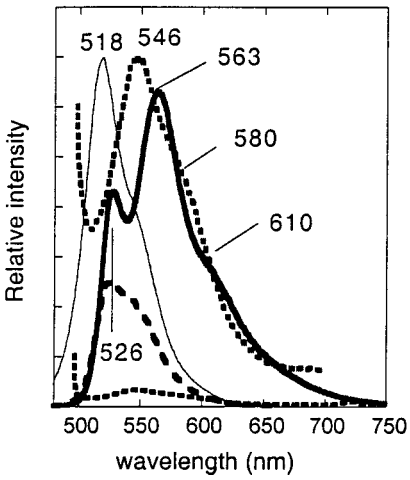

Figure 7. **P3OF-75** emission as dilute solution (solid), concentrated solution (bold dashed), solid film (dashed). The film spectrum is also normalized to better show the peak shape (thin dashed line). The normalized **P3OF-95** emision spectrum is shown as the bold solid line.

identical chromophores based on the bithiazole dimer, 5,5″-bis(2,2′-bithiazole), have quite different absorption spectra depending on the number of molecules in a unit cell.[13] This is precisely the expected effect of Davydov splitting which splits an allowed absorption in an isolated molecule into one allowed transition for each translationally nonequivalent molecule in the unit cell.[39] Conservation of momentum restricts the allowed absorptions to the transitions from the ground state to the band edges (the $k = 0$ transitions). However, this selection rule is relaxed by inclusion of phonon coupling,[40] such that the envelope of the absorption peak becomes a transform of the density of states in the exciton band structure.[36] This density of states often contains peaks centered about the vibronic levels.[40] Therefore, we ascribe the fine structure to a combination of Davydov splitting and the excitonic band structure as sampled by the phonon (vibrational) coupling. It is interesting to note that Spano et al. have calculated that these intermolecular interactions lead to a significant increase in the spectral separation of the first two vibronic peaks.[28a] It was noted above that the separations between the first two peaks in **P3OF** and **PNBO** are, in fact, larger than typical ring stretching frequencies.

Within this model, an approximate value of the Davydov splitting in **P3OF** is given by the difference in energies of the two higher energy peaks: $\Delta E = 0.15$ eV.[13] This value is similar to those found for several thiophene oligomers or polymers by absorption spectroscopy[34,35b] and by CD spectroscopy.[14c,35a] Theoretical estimates of the exciton splitting in oligothiophenes and PPV oligomers are in the range 0.10−1.0 eV.[34b,35,41]

Emission spectra of **P3OF-75** (solution and solid, $\lambda_{ex} = 457$ nm) and **P3OF-95** (solution) are shown in Figure 7. The emission spectra were independent of the excitation wavelength in the region 400−540 nm. The spectrum of **P3OF-75** was concentration dependent: the dilute solution (ca. 10^{-4} M) emitted at 518 nm with a shoulder near 540 nm. In more concentrated solution (ca. 10^{-3} M), the peak shifted to 526 nm as a result of the diminution of the 518 nm peak relative to the 540 shoulder. The emission from the film was quite weak, but

(37) (a) Hernandez, V.; Losada, S. C.; Casado, J.; Higuchi, H.; Navarrete, J. T. L. *J. Phys. Chem. A* **2000**, *104*, 661. (b) Louarn, G.; Trznadel, M.; Buison, J. P.; Laska, J.; Pron, A.; Lapkowski, M.; Lefrant, S. *J. Phys. Chem. A* **1996**, *100*, 12532. (c) Louarn, G.; Trznadel, M.; Zagorska, M.; Lapkowski, M.; Pron, A.; Buisson, J. P.; Lefrant, S. *Synth. Met.* **1997**, *84*, 579.

(38) Curtis, M. D. Submitted for publication.

(39) (a) Pope, M.; Swenberg, C. E. *Electronic Processes in Organic Crystals and Polymers*, 2nd ed.; Oxford University Press: New York, 1999. (b) Giacintov, N. E.; Swenberg, C. E. In *Luminescence Spectroscopy*; Lumb, M. D., Ed.; Academic Press: New York, 1978; p 239 ff.

(40) (a) Philpott, M. R. *J. Chem. Phys.* **1970**, *54*, 111. (b) Philpott, M. R. *J. Chem. Phys.* **1971**, *55*, 2039.

(41) Cornil, J.; dosSantos, D. A.; Crispin, X.; Silbey, R.; Bredas, J. *J. Am. Chem. Soc.* **1998**, *120*, 1289.

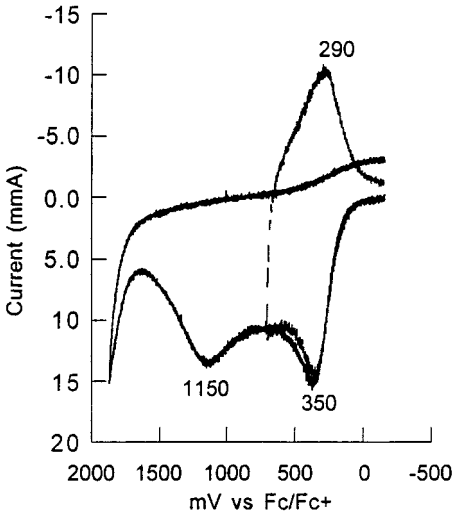

Figure 8. CV of **P3OF-75** at a 100 mV/s scan rate.

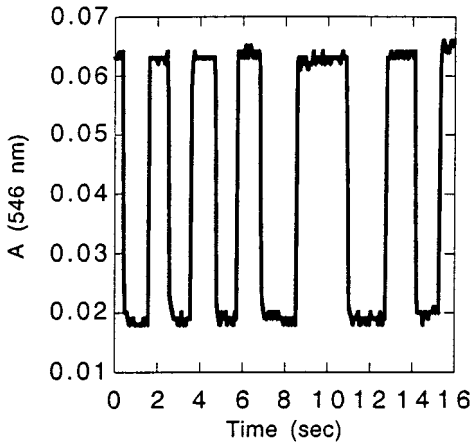

Figure 9. Absorbance at 546 nm of a thin film of **P3OF-95** on an ITO electrode vs time as the voltage is cycled between 0.0 and 700 mV (vs Ag wire reference electrode).

had a peak at 546 nm with a shoulder at 580 nm. The emission from a dilute solution of **P3OF-95** had two peaks and a shoulder at 526, 563, and 610 nm, respectively. A solid film of **P3OF-95** showed a weak, structureless emission tailing off from 560 to 750 nm. These emission spectra suggest that the **P3OF-95** chains may aggregate in solution, and the tendency to aggregate grows stronger as the degree of regioregularity increases. The high-energy edges of the emission from **P3OF-75** overlap the low-energy feet of their respective absorption peaks as expected. However, the 526 nm peak of the **P3OF-95** emission is at *higher* energy than the low energy peak in the absorption, 537 nm. This is further evidence for aggregation.[14c]

Extrapolation of the low energy edge of a graph of $(\text{abs}*h\nu)^2$ vs $h\nu$ gave a band gap of 2.21 eV for **P3OF-95** and 2.30 eV for **P3OF-75**. It is interesting to note that the oxidatively coupled poly(furan) (**PF**) prepared by Glenis et al. has a single broad peak with $\lambda_{max} = 468$ nm and a band gap of 2.35 eV,[22] i.e., the effective conjugation length of **PF** is very similar to that of **P3OF-75**.

Electrochemistry. Cyclic voltammetry was conducted on these materials to determine the possibility of n- or p-doping. Figure 8 shows a typical cyclic voltammogram, obtained on a **P3OF-75** film on a Pt electrode. All the **P3OF** samples showed a quasireversible oxidation near $E^{1/2}{}_{ox} = 0.32$ V ($\Delta E^{p}{}_{ox} = 60$ mV) vs the ferrocene/ferrocenium couple (Fc^+/Fc, 0.1 M Bu_4NPF_6 (**TBAF**) in acetonitrile supporting electrolyte). It was unexpected that the polymers have similar oxidation potentials, considering the large difference in the HOMO-LUMO gaps observed in the UV−vis spectra and the dependence of the oxidation potential on the energy level of the HOMO. However, cyclic voltammetry is complicated by many factors in the solid state, including the "break-in" potential associated with the diffusion of the electrolyte into the solid film, film thickness, adhesion to the electrode, etc.[42] For example, polyfuran films were shown to have different oxidation potentials, ranging from $E^{1/2}{}_{ox} = 0.16$ to 0.56 V (vs Fc^+/Fc),[43] depending upon the electrolyte used.[22] The oxidation potential of polyfuran with $PF_6{}^{1-}$ as the supporting electrolyte anion was reported as $E^{1/2}{}_{ox} = 0.56$ V, which is comparable to those observed for the polymers in this study.

A second, irreversible oxidation peak is observed at +1.15 V. If the potential was swept to values more positive than 1.15 V, then no reduction peak was observed on the return sweep to cathodic potentials. We believe the over-oxidized film detaches from the electrode. Two oxidation peaks are observed for regioregular **P3OT** at $E_{pa}(1) = 0.64$ V and $E_{pa}(2) = 0.91$ V.[7a,43] Thus, the first oxidation of **P3OF** is 0.32 V more facile than that of **P3OT**. It is interesting to note that PM3 calculations give values of the ionization potentials of 8.34 and 7.98 eV, respectively: for the tetramers of 3-methylthiophene and 3-methylfuran, i.e., a difference of 0.36 eV. Given the caveat concerning electrochemistry of thin films and the accuracy of the SCF-MO calculation, this agreement may be fortuitous.

Figure 9 shows the changes in absorbance at 546 nm of a thin film of **P3OF-95** on an ITO electrode immersed in the **TBAF** electrolyte as the potential is cycled between 0.0 and 0.70 V vs a Ag wire reference electrode. The color cycles between red (reduced) and black (oxidized) with a response time of about 30 ms. The relatively fast switching time may be due to the thinness of the film and, possibly, to a higher mobility of the $PF_6{}^{-1}$ counterions in the polymer caused by the presence of oxygen in the polar furan rings. The film could be cycled several hundred times with no apparent degredation, provided a dry N_2 atmosphere was maintained over the cell.

A thin film of **P3OF-95** was dip-coated onto an ITO electrode and immersed in a cell containing acetonitrile and 0.1 M **TBAF** electrolyte, a Ag-wire reference, and a Pt-wire auxiliary electrode. Figure 10 shows the spectral response at various applied voltages. Between 0.0 and 400 mV, the intensity of the peaks around 500 nm due to neutral **P3OF** decrease in intensity while a very broad peak grows in at 810 nm. At 800 mV, the 500 nm peaks continue to diminish in intensity, and the long-wavelength peak continues to grow and its maximum shifts to 775 nm. These changes are reversible (see above). Above 800 mV, the intensity of the 500 nm peaks continues to decline, and the intensity of the 775 nm peak drops into a featureless absorbance that rises to a broad peak at 1000 nm (cf. Figure 11). The changes in the spectra are fully reversible when the voltage is cycled between 0.0 and a maximum potential of about 800 mV. Above 800 mV, the intensity of the 500 nm peaks is not fully restored when the voltage is dropped back to zero. Figure 11 illustrates the lack of full reversibility when the potential was cycled to +1.2 V and then back to zero. This lack of full reversibility after cycling to higher potentials is

(42) Guay, J.; Kasai, P.; Diaz, A.; Wu, R.; Tour, J. m.; Doa, L. H. *Chem. Mater*. **1992**, *4*, 1097 and references therein.

(43) The reported potentials (vs SCE) were converted to the Fc^+/Fc reference using the standard reduction potentials vs NHE, 0.24 V (SCE) and 0.40 V (Fc^+/Fc), as reported in: *CRC Handbook of Chemistry and Physics*, 76th ed.; Lide, D. R. Editor-in-Chief; CRC: Boca Raton, FL, 1995; pp **8**-21 ff.

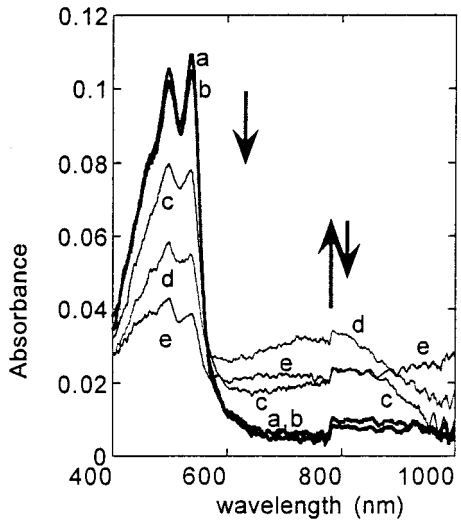

Figure 10. Spectroelectrochemistry of **P3OF-95**; applied pottential (mV) vs Ag wire reference electrode: (a) 0.0, (b) 400 (c) 600, (d) 800, and (e) 1000.

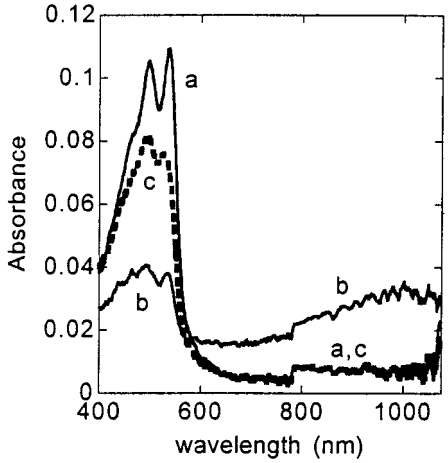

Figure 11. UV−vis−NIR spectra of **P3OF-95** as the potential was cycled from 0.0 V to 1.20 V and back to 0.0 V.

consistent with the irreversible oxidation seen in the CV curves (cf. Figure 8).

Chemical Doping and Conductivity. Thick films (5−10 μm) of **P3OF-95** and **P3OF-75** were cast from $CHCl_3$ onto quartz disks. The films were doped with I_2 vapor for a period of 3 h. The doped **P3OF-95** showed a conductivity of 1×10^{-2} S/cm^{-1} measured by both 2-point and 4-point methods. The more disordered **P3OF-75** showed a doped conductivity of 7×10^{-8} S/cm^{-1} by the 2-point probe method. Both polymers were several orders of magnitude less conductive than their thiophene counterparts,[7a] implying a lower mobility for the electronic charge carriers in the **P3OF** films. The conductivity of pristine **P3OF** films was too low to be measured with our apparatus.

The spectral changes that accompany the chemical doping are shown in Figure 12. The peaks due to the neutral polymers at 452 (**P3OF-75**) and 466−537 nm (**P3OF-95**) are replaced with new peaks at 400, 660, and 980 nm (**P3OF-75**) and at 420, 740, and 1850 nm (**P3OF-95**). The spectroelectrochemical changes seen in Figures 10, 11, and 12 are similar to those observed for a variety of conjugated polymers upon electrochemical or chemical doping and are often interpreted in terms of polarons, bipolarons, and free (metallic) electron models.[22,44] However, there is growing evidence that bipolarons may not

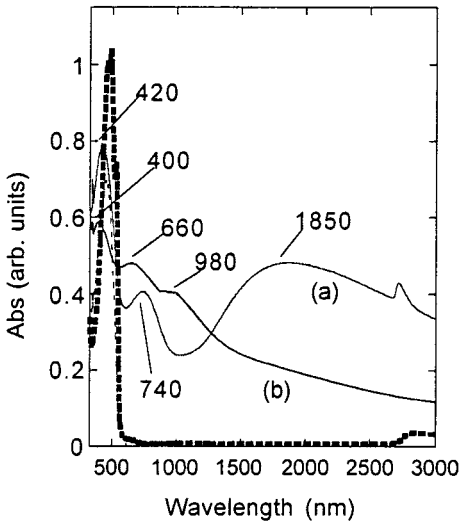

Figure 12. I_2 doped films of **P3OF-95** (a) and **P3OF-75** (b). Solid lines are the doped polymers; dashed lines are the undoped polymers (cf. Figure 6).

be stable with respect to singly charged polarons in these families of conjugated polymers.[45] The primary evidence for bipolarons is the rapid decrease in concentration of unpaired spins or magnetic susceptibility with increasing doping levels, but Miller et al. have recently shown that polarons (singly charged, radical cations) are readily spin-paired by co-facial interactions of their π-systems.[46] Brocks has published ab initio calculations that show the disproportionation of two singly charged polarons into a neutral molecule and a bipolaron is endothermic.[47] Previous calculations in which the disproportionation is exothermic have used a Hamiltonian with a higher lattice stabilization energy for the bipolaron.

The spin-paired polaron model of Miller et al.[46b] gives also an explanation for the spectral changes shown in Figures 11 and 12 and accounts for the different behavior of the regioregular and -irregular polymers. Removal of an electron from the HOMO and formation of a π-dimer creates two new $\pi-\pi$ transitions in addition to a HOMO-LUMO transition that remains near in energy to that of the original $\pi-\pi^*$ transition of the neutral molecule as shown in Figure 13. One of the new bands corresponds to a HOMO-1 to HOMO transition and is expected to be lower energy than the $\pi-\pi^*$ transition of the neutral molecule. The second new band arises from a transition between states that are formed from the in-phase or out-of-phase combinations of the HOMO on the two molecules comprising the dimer. This band will have a relatively low energy because the intermolecular interactions involve rather small overlaps between neighboring π-systems. In a crystalline, π-stacked polymer, the intermolecular interactions could lead to bands of energy levels as shown on the right side of Figure 13. In a one-dimensional stack, a Peierls distortion, characterized by a long−short alternation in intermolecular distances (stacking of dimers), will open a gap in the half-occupied band that arises from the

(44) (a) Bredas, J. L.; Thémans, B.; Fripiat, J. G.; André, J. M.; Chance, R. R. *Phys. Rev. B* **1984**, *29*, 6761. (b) Soos, Z. G.; Galvao, D. S. *J. Phys. Chem.* **1994**, *98*, 1029. (c) Curtis, M. D.; Cheng, H.; Nanos, J. I.; Nazri, G.-A. *Macromolecules* **1998**, *31*, 205.

(45) (a) Hong, Y.; Miller, L. L. *Chem. Mater.* **1995**, *7*, 1999. (b) Duan, R. G.; Miller, L. L.; Tomalia, D. A. *J. Am. Chem. Soc.* **1995**, *117*, 10783. (c) Bach, C. M.; Reynolds, J. R. *J. Phys. Chem.* **1994**, *98*, 13636. (d) Sato, M.; Hiroi, M. *Synth. Met.* **1995**, *69*, 307.

(46) (a) Hill, M. G.; Penneau, J. F.; Zinger, B.; Mann, K. R.; Miller, L. L. *Chem. Mater.* **1992**, *4*, 1106. (b) Graf, D. D.; Duan, R. G.; Campbel, J. P.; Miller, L. L.; Mann, K. R. *J. Am. Chem. Soc.* **1997**, *119*, 5888.

(47) Brocks, G. *Synth. Met.* **1999**, *102*, 914.

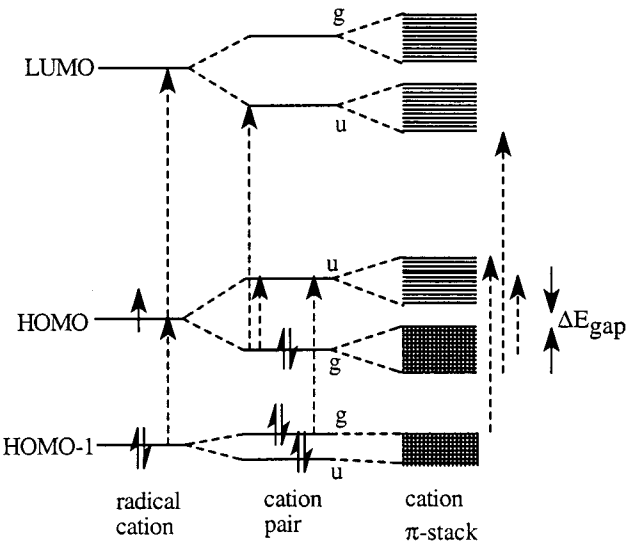

Figure 13. Evolution of polaron (radical cation) energy levels as the main chain π-stacks. The labels "g" and "u" refer to the inversion symmetry of the wave functions for levels in an H-type aggregate. The labels would be reversed for a J-type aggregate.

singly occupied molecular HOMO. We will refer to this split band as the "conduction band". A transition from evenly spaced intermolecular distances to a stacking of dimers has been observed experimentally by Miller et al.[46b]

With this energy scheme, we therefore assign the band at 420 nm in the spectrum of I_2-doped **P3OF-95** to the "HOMO-LUMO" transition, the 740 nm peak to the HOMO-1 to conduction band transition, and the broad absorption from 1500 to 3000 (peak about 1850) nm to transitions within the conduction band. The development of a conduction band is not possible unless the molecules can form an extensive π-stacked structure. The spectrum of **P3OF-75** shows only a weak tailing off of the absorption to longer wavelengths (Figure 12b). This is what is expected if there is no regular or extensive π-stacking in the solid-state structure. In **P3OF-75**, about 16% of the diads have more than five rings with sequential HT-links before an HH or TT interruption, as compared to 47% of the diads in **P3OF-95**.[38] Thus, even in **P3OF-75**, there will be some regions where the longer sequences of HT-linkages can form stacks of dimers, trimers, etc., giving rise to a dispersion of low energy transitions with intensity falling off into the NIR. The spectrum of I_2-doped **P3OF-75** is therefore interpreted as a composite of the spectra of a mixture of "oligo-polarons", and the various peak positions depend on the relative proportions of the oligomeric species. An extrapolation of $(\text{abs}^*h\nu)^2$ vs $h\nu$ in the region 2500−3000 nm gave a value of 0.34 eV for the conduction band gap in I_2-doped **P3OF-95.** The comparable value for **P3OF-75**, obtained from the absorption in the region 1000−1400 nm, is 0.9 eV, although a small fraction of the sample has a lower band gap as evidenced by the gradual tailing of the absorption to long wavelength.

Stability. The thermal stability of the three samples, **P3OF-95**, **-75**, and **-50**, was tested by thermal gravimetric analysis (TGA). Figure S6 shows the TGA traces for the three polymers heated under a N_2 atmosphere. A 5% weight loss was observed at 380, 320, and 275 °C for **P3OF-95**, **-75**, and **-50**, respectively. Thus, the more regular polymers are more stable thermally. Differential Scanning Calorimetry (DSC) was also performed on all polymers, but no transitions were observed up to 200 °C.

The environmental stability of **P3OF-95** was studied by FT-IR and UV−vis over time. It was noticed that films of red

Scheme 4

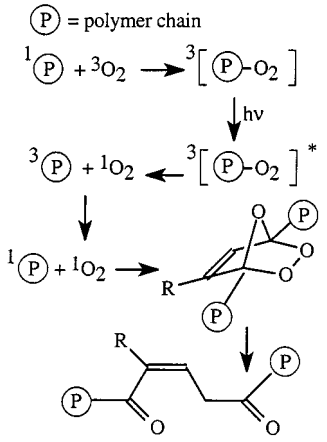

P3OF-95 bleached over a period of hours to days. To determine the cause of bleaching, eight thin films were cast on glass slides. Each slide was placed in an environmental chamber in which eight different combinations of ambient room light or dark, nitrogen or air atmosphere, and dry or 100% humidity conditions could be produced. Of the eight samples, only the two exposed to both ambient light and air had bleached; humidity had no effect on the course of this light-induced oxidation (Figure S2). The bleached film had a peak in the UV with a λ_{max} of 294 nm (Figure S3).

Figure S4 overlays the FT-IR spectra of both **P3OF-95** and **P3OF-50**. The polymers give rise to the same bands with variations in the relative intensities of each band. The FT-IR peaks observed for the polymers were ν = 801, 921, 1026, 1096, 1265, 1400, 1455, 1537, 1631, 1652, 1729, 2852, 2924, 2959, and 3047 cm^{-1}. Figure S7 shows the FT-IR spectra of a fresh and a light/air-bleached **P3OF-95** film. The peaks at 802, 921, 1537, and 1631 cm^{-1} decreased in intensity as the film became bleached, and a peak grew in at 1773 cm^{-1}, assigned to an ester/α,β-unsaturated ketone derivative (Scheme 4). The unsaturated ester is postulated to form via the ring-opening of a furan endoperoxide, known to form in high yield from the reaction of singlet oxygen with 2,5-substituted furans.[48] Abdou et al. reported the oxidation of P3HT by photogenerated singlet oxygen and proposed the formation of $^1O_2$ via a charge-transfer complex between O_2 and the polymer as shown in Scheme 4.[6] Our experience with **P3AT**s shows that **P3OF** is photobleached much more rapidly than the former. Films of **P3AT**s remain colored for months if not years when allowed to stand in the laboratory under normal fluorescent lighting. In contrast, **P3OF** films bleach in a matter of days to weeks under similar conditions. In air, the polymers degrade rapidly at 200 °C as evidenced by the bleaching of the UV−vis spectrum (Figure S5), but the unsaturated ester apparently is not formed in the thermal oxidation since the UV peak at 294 nm is absent.

Conclusions

A new series of regioregular and regioirregular heterocyclic, conjugated polymers has been developed based on furan instead of the more popularly studied thiophene polymers. The furans showed many of the same trends and features as found in poly(3-octylthiophene), e.g., the dependence of crystalline morphology on the side chain stereochemistry, and the effects the solid-state morphology on UV−vis−NIR spectra and conductivity. The I_2-doped poly(furans) were several orders of magnitude less

(48) (a) Gollnick, K.; Griesbeck, A. *Tetrahedron* **1985**, *41*, 2057. (b) Adam, W.; Eggelte, H. J.; Rodriguez, A. *Synthesis* **1979**, 383.

conductive than poly(thiophenes), most likely as a result of electronic effects of the oxygen, since both systems are structurally similar. A comparison of the spectra of I_2-doped **P3OF-95** and **P3OF-75** suggests that the polaron energy levels develop into well-defined bands as a result of good π-stacking. Compared to poly(3-alkylthiophenes), the more polar poly(furans) are somewhat less soluble in $CHCl_3$ resulting in aggregation as evidenced by the fine structure in the UV−vis solution spectrum of **P3OF-95** that resembles the solid-state spectrum. The poly(furans) showed limited stability toward a combination of light and oxygen, an issue that would need to be addressed if these polymers are to be used in electronic devices.

Acknowledgment. This research was supported by the National Science Foundation (DMR-9510274 and DMR-9986123).

Supporting Information Available: Figures S1−S3 and S5 showing the UV−vis spectra of **P3OF** under various treatments as described in the text, Figure S4, the IR spectra of **P3OF-95** and **P3OF-50**, Figure S6 showing the TGA of the three **P3OF**s, and Figure S7 showing the IR spectrum of the thermally oxidized **P3OF** (PDF). This material is available free of charge via the Internet at http://pubs.acs.org.

JA003588I